Available online at www.sciencedirect.com
SCIENCE DIRECT®
Thin Solid Films 453–454 (2004) 496–500
thin solid films
www.elsevier.com/locate/tsf

Laser ablation of iron by ultrashort laser pulses

N.N. Nedialkov[a], S.E. Imamova[a], P.A. Atanasov[a,*], G. Heusel[b], D. Breitling[b], A. Ruf[b], H. Hügel[b], F. Dausinger[b], P. Berger[b]

[a]*Institute of Electronics, Bulgarian Academy of Sciences, 72, Tsarigradsko Shose, Sofia 1784, Bulgaria*
[b]*Institut für Strahlwerkzeuge, Universität Stuttgart, 43 Pfaffenwaldring, 70569 Stuttgart, Germany*

Abstract

Laser ablation of iron is investigated experimentally and theoretically. The experiments are performed by Ti:sapphire laser at pulse duration $\tau_p = 0.1$ ps. The ablation rate and the surface structures are determined. Different regimes of the process at low and high laser fluences are observed. At fluences above several joules per square centimeter, the ablation is accompanied by the formation of significant amount of molten material. Molecular dynamics simulation technique is used to describe the process. Different mechanisms of material ejection are observed. The role of the electron heat diffusion in the process of dissipation of the energy is also estimated. Good coincidence is obtained between the model and experimental results.

PACS: 79.20.Ds; 02.70.Ns

Keywords: Ultrashort laser ablation; Molecular dynamics simulation; Iron

1. Introduction

The femto- and picoseconds laser systems have found a great application during recent years [1–4]. The fast energy deposition determined by application of ultrashort laser pulses results in a high spatial energy concentration into the material and as consequence reduction of the heat-affected zone and the presence of the liquid phase. These led to the decrease of ablation threshold and makes precise micro-processing and structuring of almost any kind of materials possible. Furthermore, the ejection of material occurs mainly after the laser–pulse interaction and any effects of absorption and scattering of the laser radiation in the plasma can be excluded with the exception of high rep rate processing and drilling holes having high aspect ratio.

As a base mechanism in a large number of applications for laser processing—cutting, drilling, surface cleaning, etc., the ultrashort laser ablation has been the object of many experimental [1–9] and theoretical [7,10–12] investigations. It was found that the process is very complicated, it depends on the processing conditions and the material properties, and its description should take into account optical absorption, heat conduction, phase transitions, fluid dynamics and evaporation kinetics. Furthermore, the presence of non-linear processes in the absorption of the laser energy and ultra fast order–disorder transitions related to the high excitation of the electron component also should be considered. The mechanism of ablation process has been analyzed on the basis of different models—thermal [13,14], thermo-mechanical [15], photochemical, and defects' models [16]. Generally, it is considered that the energy is deposited in the material faster than it can be dissipated by the classical channels of relaxation, i.e. thermal or mechanical, and an overheating of the system can be realized, which will develop a critical pressure gradient. Furthermore, at certain conditions, the laser energy can cause direct bond breaking and ejection of single atoms, molecules or clusters. Depending on the processing conditions certain mechanisms could be considered as dominant, but a more general description should take into account simultaneous participation of several mechanisms involved.

In this work, ultrashort laser ablation of iron is investigated experimentally and theoretically. Fe is chosen as a metal with very broad industrial application.

*Corresponding author. Fax: +359-2-9753201.
E-mail address: paatanas@ie.bas.bg (P.A. Atanasov).

0040-6090/04/$ - see front matter © 2003 Elsevier B.V. All rights reserved.
doi:10.1016/j.tsf.2003.11.112

Table 1
Parameters of Fe used in the model

λ (nm)	R (%)	α (cm^{-1})	$1/\alpha$ (nm)	T_m (K)	T_v (K)
800	65	0.54×10^6	18.5	1811	3145

Molecular dynamics simulation is used for description of the ultrashort laser ablation.

2. Experimental setup

Ti:sapphire laser system (Spectra Physics Hurricane) is used in the experiments. It is based on the chirped—pulse amplification technique and continuous variation of the pulse duration, τ_p, from 0.1 to 6 ps is available. The experiments are performed at $\tau_p=0.1$ ps. The pump is made by 1 kHz rep rate SHG Nd:YAG laser. The desired number of pulses is controlled by fast mechanical shutter. Laser radiation is focused on the material surface by lens having 100-mm focal length. The focal spot size at FWHM is 18 μm. The targets are 0.5 mm thick 99.5% pure Fe plates, placed in vacuum chamber at a pressure of 1 mbar air. Laser scanning microscope (LSM) is used to observe the ablated area and to measure the ablation depth. The ablation depth per pulse is evaluated by measuring of the total depth of the hole drilled divided by the number of pulses used.

3. Simulation details

Molecular dynamics (MD) simulation technique [17] is applied to investigate the ablation of iron. The pair Morse potential governs the interaction between atoms in the system. Velocity Verlet algorithm [17] is used to integrate the equation of motion. Periodic boundary conditions are imposed in x and y directions to describe the infinite medium and velocity dampening techniques are applied at the bottom of the simulated system in order to minimize the effects of reflection of the shock wave. Simulation system is formed by $15\times15\times105$ (175) body–centered unit cells and has dimensions of $4.3\times4.3\times30$ (50) nm^3. The simulations are made for $\tau_p=0.1$ ps laser pulse at $\lambda=800$ nm as in the experiments. The laser beam intensity is considered spatially uniform and has Gaussian temporal distribution. The parameters of Fe used in the calculations are given in Table 1. They are assumed to be constant during the simulation time interval.

The number of photons, corresponding to the laser energy, is deposited in the material exponentially following the Lambert–Beer's law. The energy of the photons is transferred to the atoms of the system within a characteristic time τ_{eq}, corresponding to the time of electron-lattice energy transfer and the establishment of the equilibrium temperature. The energy deposited to the atoms in the system contributes to the increase of their kinetic energy. More detailed description of the simulation model is given elsewhere [18].

The effects of the electron thermal diffusion are taken into consideration by an increase of the effective depth of the penetration of the laser energy. This depth is estimated by the electron thermal diffusion length $l_{th}^e\approx(D_e\tau_{eq})^{1/2}$ ($D_e=K_e/C_e$ is the electron diffusion coefficient). Due to the lack of data for the electron thermal conductivity K_e and the electron heat capacity C_e for Fe and their dependences on the temperature, they are estimated based on the data available for other metals given in Ref. [19] and corrected in order to obtain better coincidence with the experimental values for the ablation depth.

4. Results and discussions

The ultrashort laser ablation is investigated experimentally in the range of laser fluences from the threshold up to 100 J/cm^2. Fig. 1 represents ablation depth per pulse as a function of the laser fluence. As one can see, different regimes of ablation can be defined. At low laser fluences (from the threshold estimated to be approximately 100 mJ/cm^2 up to several hundreds of mJ/cm^2) the ablation depth slightly increases with the laser fluence rise. The ablation rate in this range is confined to several tens of nanometers per pulse. Further increase of the laser fluence results in a steep rise of the ablation depth. Higher than 20 J/cm^2 it exceeds 1 μm per pulse. The change of the ablation rate is also accompanied by a variation of features of the ablated region. Fig. 2 shows LSM images of the ablated holes at (a) 0.3 J/cm^2, 100 laser pulses; (b) 10 J/cm^2, 10 pulses; and (c) 100 J/cm^2, 10 pulses. No trace of molten material is observed at fluences near the threshold. However, the presence of molten phase is clearly

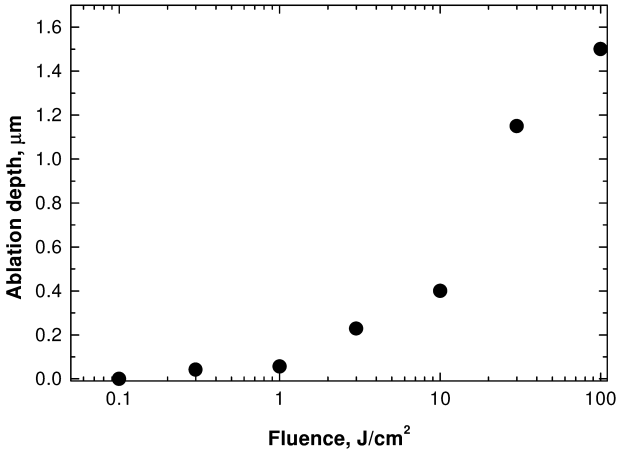

Fig. 1. Ablation depth as a function of the laser fluence in Fe. $\tau_p=$ 0.1 ps, $\lambda=800$ nm.

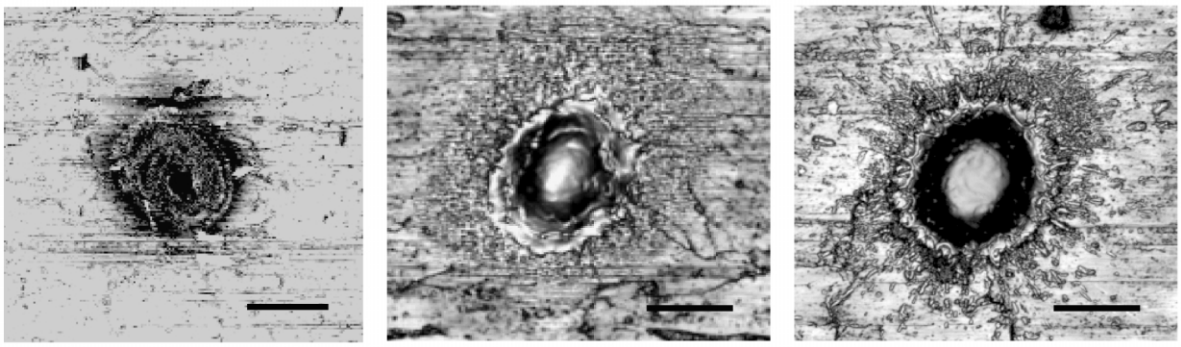

Fig. 2. LSM images of ablated holes in Fe: (a) $F=0.3$ J/cm^2, 100 pulses; (b) $F=10$ J/cm^2, 10 pulses; (c) $F=100$ J/cm^2, 10 pulses. $\tau_p=0.1$ ps, $\lambda=800$. The black mark corresponds to 15 μm.

expressed at 10 J/cm^2, while at 100 J/cm^2 big liquid droplets can be observed around the hole.

The different mechanisms of ablation could be referred to the contribution of the electron thermal diffusion in the process of dissipation of the laser energy [20]. At high laser fluences the number of hot electrons is sufficient to cause increase of the depth of interaction compared to the optical penetration one. This may lead to an increase of the ablation depth.

In order to clarify the processes involved in the ablation, we apply MD simulation model. At laser fluences near to the threshold ablation is realized through ejection of single atoms and small clusters. The material is evaporated and negligible molten phase is observed. However, the increase of the laser fluence results in quite different feature of ejection process. Fig. 3 represents evolution of the ablation process in Fe at laser fluence of $F=0.5$ J/cm^2. The transfer of the energy in the thermal motion of the atoms in the system results in fast rise of the temperature in the absorbing volume. Several picoseconds after the laser pulse onset the material is overheated as the temperature is approximately 5000 K in the surface region (Fig. 4). The overheated material expands rapidly with a velocity in order the of 3.5 km/s and approximately 4 ps after laser pulse offset density fluctuation are observed. Later, the ablated material decomposes into single particles, clusters and liquid droplets. These features of the process evolution indicate participation of the mechanism of phase explosion in the ablation [7,14]. Furthermore, the

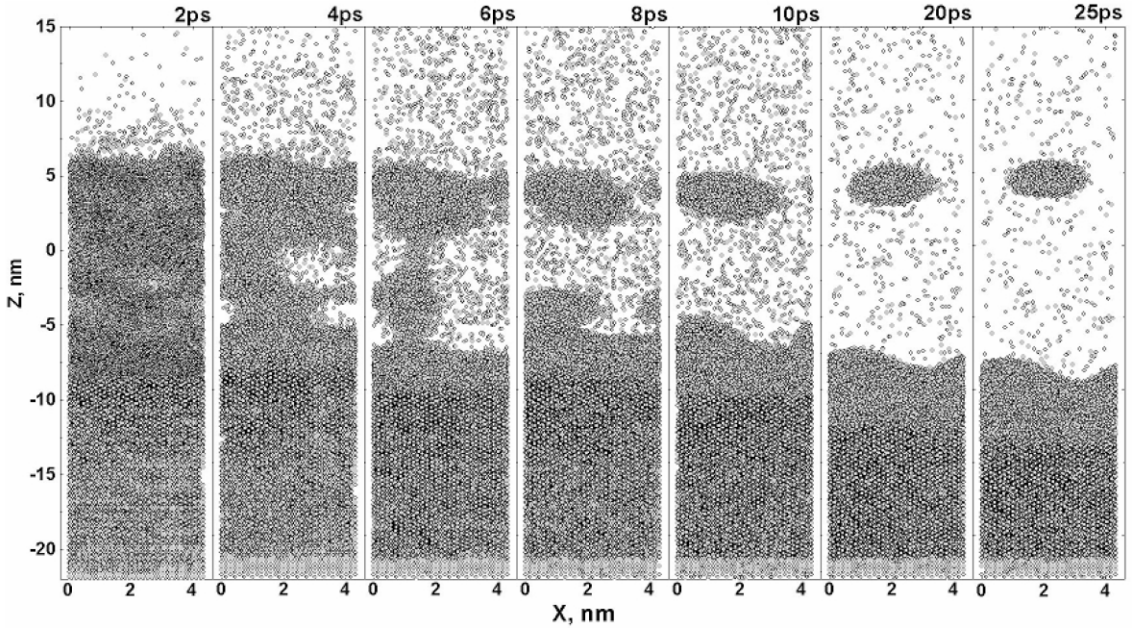

Fig. 3. Evolution of the ablation process in Fe. $F=0.5$ J/cm^2, $\lambda=800$ nm, and $\tau_p=0.1$ ps.

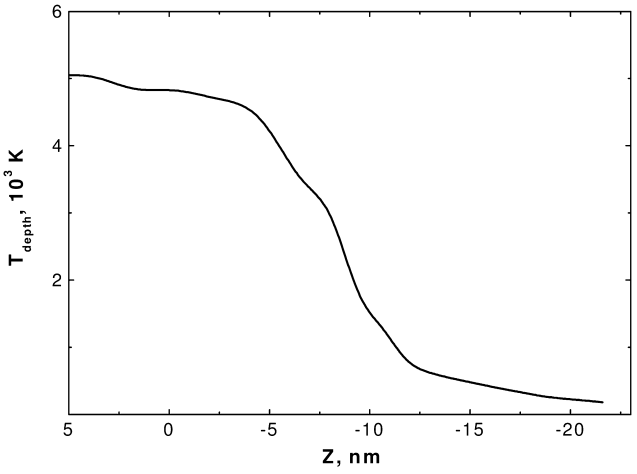

Fig. 4. Temperature distribution as a function of the depth at 3 ps after the laser pulse onset. $F=0.5$ J/cm^2, $\tau_p=0.1$ ps, $\lambda=800$ nm.

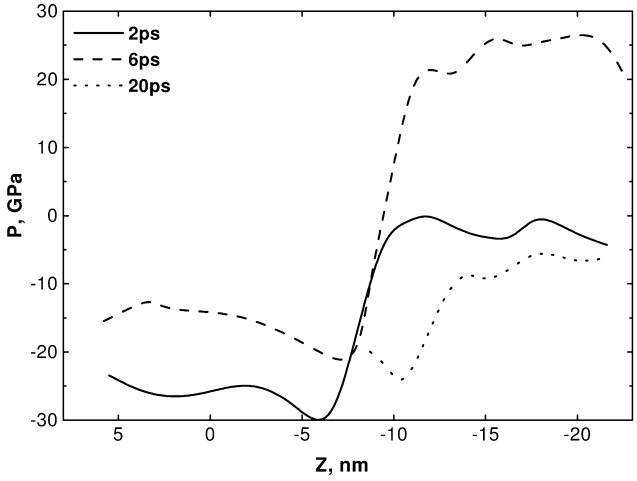

Fig. 5. Depth distribution of the pressure at different moments. $F=$ 0.5 J/cm^2, $\lambda=800$ nm, and $\tau_p=0.1$ ps.

presence of molten phase is clearly expressed by disordered structure in the surface region. The explosion-like ejection of particles observed leads to the formation of strong recoil pressure, which can expel existing molten material. Further increase of the laser fluence leads to stronger overheating and rise of the amount of molten phase. The latter is connected to the contribution of the electron heat diffusion. The inclusion of the mechanism of melt ejection in the ablation process can also explain the observed decrease of the ablation rate with the rise of the depth (number of applied laser pulses) in the material. The surface micro-relief changes significantly due to the recast layer even after one single pulse.

Due to the fast energy deposition ensured by the ultrashort laser pulses, the heat is localized into near constant volume of the material, which develops strong pressure. Fig. 5 represents the distribution of the pressure in depth of the material at different moments after the laser pulse onset. The conditions are as in Fig. 3. The positive pressures express the compression and negative, the tension in the material, respectively. As one can see the compression exceeds a value of 25 GPa at 6 ps after laser pulse impact. The position of the maximum of the tension wave at 2 ps corresponds to the depth, where the material rends and the new surface is formed. All these features can be referred to a presence of a thermomechanical mechanism involved in the ablation phenomenon. The compression wave formed in the material can also cause changes in the material structure. Fig. 6 shows the structure of the iron taken in depth of 15 nm at 6 ps after the laser pulse onset. The laser fluence is 2 J/cm^2 (Fig. 6a). The structure is obtained from the configuration of the atoms in x–y plane in the layer having thickness of 1 nm. The temperature in this layer is estimated to be 1200 K. The structure of unaffected initial lattice at 300 K is also shown (Fig. 6b) for comparison.

The accuracy of the MD modeling is verified by comparison of the ablation depth with the experimental data obtained. Fig. 7 shows the dependence of the ablation depth per pulse on the laser fluence. As one can see, there is good agreement between the MD and

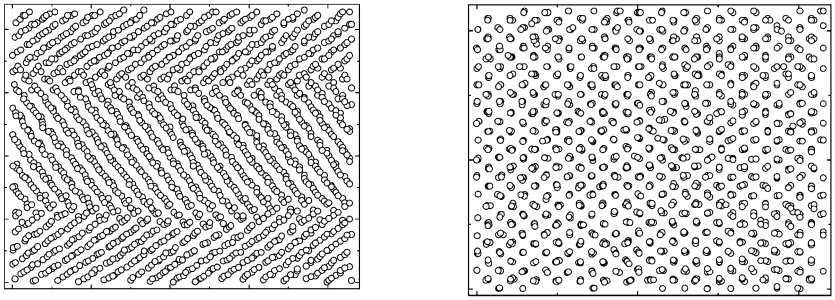

(a) (b)

Fig. 6. Structure of Fe taken in depth of 15 nm at 6 ps after the interaction of laser pulse at $F=2$ J/cm^2 (a), (b) the initial structure of Fe. The structures are obtained from the configuration of the atoms in x–y plane in the layer with thickness of 1 nm.

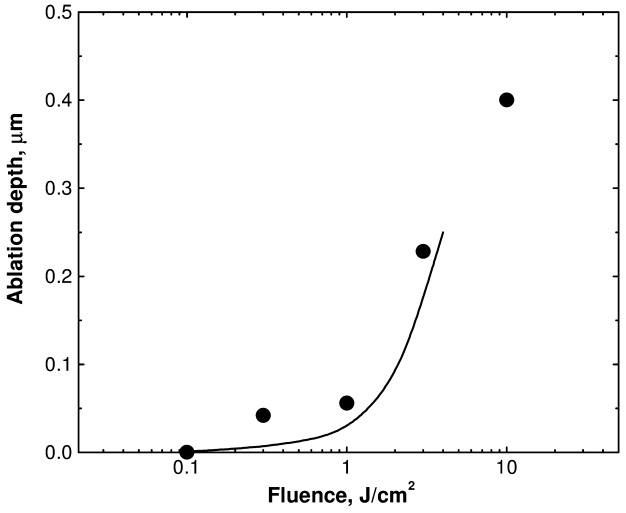

Fig. 7. Ablation depth as function of the laser fluence: dots–experimental data, line–MD simulation results. $\lambda = 800$ nm and $\tau_p = 0.1$ ps.

experimental values. The observed discrepancy could be referred to the lack of knowledge of the reliable data for the thermo-physical parameters of the electron system and, therefore, the rough estimation of the electron thermal diffusion length.

5. Conclusions

The process of ablation of iron with 0.1 ps laser pulse is investigated experimentally and theoretically. Different mechanisms of ablation are responsible for the ejection of the material depending on the laser fluence. At low fluences the ablation is realized through evaporation and single atoms and small clusters are expelled. The increase of the laser fluence results in inclusion of several mechanisms of material ejection, which have to be considered to take part in the process simultaneously. The fast energy deposition ensured by the femtosecond laser pulses, causes strong overheating of the absorbing volume. Several picoseconds after the laser pulse impact the material are ejected explosively. Due to the electron thermal conductivity a large amount of molten material is formed and expelled by the recoil pressure. The process of ablation is also accompanied by the formation and propagation of compression and tension waves, which can cause changes of the structure of the material. It should be pointed out that some non-thermal mechanisms related to the strong excitation of the electron system observed in ultrashort laser pulses-material interactions, also can take part in the process. The investigations in this line are planed as a future work.

Acknowledgments

This work is supported financially in part by the BMBF project No 13N7710/6 (PRIMUS), Germany and by the Bulgarian National Science Foundation under contract F-1209.

References

[1] X. Zhu, A.Yu. Naumov, D.M. Villeneuve, P.B. Corkum, Appl. Phys. A 69 (1999) S367.
[2] M.K. Kim, T. Takao, Y. Oki, M. Maeda, Jpn. J. Appl. Phys. 39 (2000) 6277.
[3] J.-H. Klein-Wiele, G. Marowsky, P. Simon, Appl. Phys. A 69 (1999) S187.
[4] B. Le Drogoff, F. Vidal, Y. von Kaenel, M. Chaker, T.W. Johnston, S. Laville, M. Sabsabi, J. Margot, J. Appl. Phys. 89 (2001) 8247.
[5] S. Preuss, A. Demchuk, M. Stuke, Appl. Phys. A 61 (1995) 33.
[6] S. Nolte, C. Momma, H. Jacobs, A. Tünnermann, B.N. Chichkov, B. Wellegehausen, H. Welling, J. Opt. Soc. B 14 (1997) 2716.
[7] D. Perez, L. Lewis, Phys. Rev. Let. 89 (2002) 255504.
[8] M. Hashida, A. Semerok, O. Gobert, G. Petite, J.-F Wagner, Proc. SPIE 4423 (2001) 178.
[9] M. Hashida, A. Semerok, O. Gobert, G. Petite, Y. Izawa, J.-F Wagner, Appl. Surf. Sci. 197-198 (2002) 862.
[10] D. von der Linde, K. Sokolowski-Tinten, Appl. Surf. Sci. 154 (2000) 1.
[11] L.V. Zhigilei, P.B.S. Kodali, B.J. Garrison, J. Phys. Chem. B 102 (1998) 2845.
[12] L.V. Zhigilei, Appl. Phys. A 76 (2003) 339.
[13] E. Ohmura, I. Fukumoto, Int. J. Jpn. Soc. Prec. Eng. 30 (1996) 128.
[14] L.V. Zhigilei, B.J. Garrison, Appl. Phys. A 69 (1999) S75.
[15] L.V. Zhigilei, Appl. Phys. A 76 (2003) 339.
[16] M. Lenzner, F. Krausz, J. Krüger, W. Kautek, Appl. Surf. Sci. 154–155 (2000) 11.
[17] M.P. Allen, D.J. Tildesley, Computer Simulation of Liquids, Clarendon Press, Oxford, 1987, pp. 71–108.
[18] N.N. Nedialkov, S.E. Imamova, P.A. Atanasov, A. Ruf, P. Berger, F. Dausinger, submitted for publication.
[19] S.-S. Wellershoff, J. Hohlfeld, J. Güdde, E. Matthias, Appl. Phys. A 69 (1999) S99.
[20] S. Nolte, C. Momma, H. Jacobs, A. Tünnermann, B.N. Chichkov, B. Wellegehausen, H. Welling, J. Opt. Soc. B 14 (1997) 2716.